Version of Record: https://www.sciencedirect.com/science/article/pii/S1568988319301799
Manuscript_f621055c27f8e271e3c4431817cf6166

An extraordinary *Karenia mikimotoi* "beer tide" in Kachemak Bay Alaska

Mark Vandersea[1], Patricia Tester[2], Kris Holderied[3], Dominic Hondolero[3], Steve Kibler[1], Kim Powell[3], Steve Baird[4], Angela Doroff[5], Darcy Dugan[6], Andrew Meredith[7], Michelle C. Tomlinson[8], Wayne Litaker[1]

[1]National Oceanographic and Atmospheric Administration, National Ocean Service, Centers for Coastal Ocean Science, Stressor Detection and Impacts Division, Beaufort Laboratory, Beaufort, NC 28516

[2]Ocean Tester, LLC, 381 Gillikin Road, Beaufort, NC 28516

[3] National Oceanographic and Atmospheric Administration, National Ocean Service, Centers for Coastal Ocean Science, Kasitsna Bay Laboratory, Homer, AK

[4] Kachemak Bay National Estuarine Research Reserve, Homer, AK

[5]South Slough National Estuarine Research Reserve, Charleston, OR

[6]Alaska Ocean Observing System, Anchorage, AK

[7]Consolidated Safety Services, Inc. Fairfax, VA

[8]National Oceanographic and Atmospheric Administration, National Ocean Service, National Centers for Coastal Ocean Science, Silver Spring, MD

Abstract

In autumn of 2013 an immense dinoflagellate bloom developed in Kachemak Bay, AK, USA. Much of the Bay was discolored a dark amber color and raised public concerns as small scale fish kills were reported in a few locations. Light microscopy revealed a monospecific bloom of gymnodinoid dinoflagellates that were previously unknown from the Bay. Gene sequencing of SSU rDNA from cells collected from the bloom confirmed the causative species to be *Karenia mikimotoi*. This represents the first report of a *K. mikimotoi* bloom in Alaska. After the bloom organism was confirmed, a *K. mikimotoi* species-specific qPCR assay was developed and used to assess *K. mikimotoi* abundances in DNA extracted from phytoplankton samples from Kachemak Bay and Lower Cook Inlet (LCI) obtained over a six-year period. The *K. mikimotoi* abundances were compared with corresponding time series of environmental variables (water temperature, salinity, water column stability, nutrients, precipitation and wind speed) to assess the environmental factors contributing to the development of the bloom. The results showed early bloom development occurred in August when snow melt reduced salinities and increased water column stability during a period of calm winds. Peak bloom concentrations occurred in late September (10^7 cell eq. L^{-1}) even as water temperatures were decreasing. The bloom gradually declined over the winter but persisted until April of 2014. *Karenia mikimotoi* cells were not detected two years prior or three years following the bloom, suggesting cells were introduced to Kachemak Bay at a time when conditions allowed *K. mikimotoi* to thrive.

Introduction

In September of 2013 an unusual and immense dinoflagellate bloom in Kachemak Bay, AK caused the water in much of the Bay to be a dark amber color with reports of tinted seafoam.

There was heightened public concern over the immensity of the bloom as well as small scale fish kills that were reported. The color and increased foam on the water led local residents to term the phenomenon the "beer tide". Light microscopy observations revealed a monospecific bloom of an unknown dinoflagellate that prompted additional efforts to resolve the species' identification. Molecular methods (PCR) were used to confirm that the dinoflagellate was *Karenia mikimotoi*, a toxic dinoflagellate with a cosmopolitan distribution and a commonly reported red tide species. First described from Japan in 1935, *K. mikimotoi* has also been reported from the western English Channel, the coastal waters of Norway, Ireland, Scotland, Hong Kong, China, Australia, New Zealand, western India, and the United States (Oda, 1935; Chang, 1996; Nakamura et al., 1996; Raine et al., 2001; Lu and Hodgkiss, 2004; Silke et al., 2005; Davidson et al., 2009; Al-Kandari et al., 2011; Robin et al., 2013; PIRSA, 2014; Barnes et al., 2015; Lin et al., 2015; O'Boyle et al., 2016; MDMR, 2017). The cells are not toxic to humans but have caused fish and benthic invertebrate mortalities resulting in major economic losses in some cases (Lu and Hodgkiss, 2004; Mitchell and Rodger, 2007; Davidson et al., 2009; Robin et al., 2013; PIRSA, 2014). Toxic and hemolytic compounds such as gymnocins and hemolytic glycolipids have been extracted from cultured cells, however, the mechanism of toxicity remains unknown (Satake et al., 2002; Satake et al., 2005; Mooney et al., 2011; Shi et al., 2012).

The *Karenia mikimotoi* bloom occurred during an ongoing long-term project to assess the distribution and abundance of *Alexandrium catenella* in lower Cook Inlet conducted by NOAA, the Gulf Watch Alaska monitoring program (http://www.gulfwatchalaska.org/monitoring) and the phytoplankton monitoring network maintained by the Kachemak Bay National Estuarine Research Reserve (KBNERR) (Vandersea et al., 2018). Phytoplankton samples for that study

were collected in Katchemak Bay over a six-year period (2011–2017). The existence of these samples made it possible, along with development of a species-specific qPCR assay, to determine *Karenia mikimotoi* cell concentrations in water samples collected before, during, and after the bloom. By comparing the *K. mikimotoi* cell concentrations to time series of environmental data routinely collected by KBNERR, we were able to investigate factors associated with bloom development. The qPCR assay targeted the ITS2 region of the rRNA gene complex and employed standard curves that were constructed using known concentrations of cultured cells as well as diluted PCR amplicons containing the assay's target sequence. It should be noted that other quantitative molecular *K. mikimotoi* assays have been published and were similarly employed in those studies (Yuan et al., 2012; Smith et al., 2014; Eckford-Soper and Daugbjerg, 2015; Engesmo et al., 2018). The qPCR assay used in this study was sufficiently sensitive to determine if *K. mikimotoi* was present at background concentrations in Kachemak Bay year around as a normal component of the phytoplankton community. It also allowed us to document the timing of bloom initiation, occurrence of peak abundances, and the bloom duration in relation the environmental conditions that occurred in Kachemak Bay.

2. Materials and Methods

2.1 Lower Cook Inlet and Kachemak Bay sampling locations, phytoplankton sampling procedures, nutrient and chlorophyll measurements, oceanographic and meteorological data collection

The 2013 *Karenia mikimotoi* bloom in Kachemak Bay, AK occurred during an ongoing long-term project to assess the distribution and abundance of *Alexandrium catenella* in lower Cook Inlet (Vandersea et al., 2018). Phytoplankton samples and environmental data for that

study were collected over a six-year period (2011–2017) and were also used in the current study. The majority of the data that we present in the current study was collected between 2012–2015 from the locations and transects shown in Figure 1. Data collected from stations in lower Cook Inlet were pooled and analyzed collectively to characterize *K. mikimotoi* cell abundances and environmental conditions outside of Kachemak Bay and included Transects 3, 6, and 7 (Fig. 1B). Similarly, data collected from stations inside Kachemak Bay also were pooled to characterize cell abundances and environmental conditions inside Kachemak Bay and included Transects 4, 9, Kasistna Bay Laboratory, and Jakoloff Bay Dock (Fig. 1C). For water sampling, ten to forty liters of surface water containing live phytoplankton were collected at each station using a bucket and concentrated with a 20 μm mesh plankton net. The resulting concentrate was shaken gently to homogenize the sample and a 125 mL aliquot was preserved with neutral Lugol's iodine solution for molecular analyses (Auinger et al., 2008) and then shipped to the National Oceanic Atmospheric Administration's (NOAA) Beaufort Laboratory in Beaufort, NC. DNA was extracted from the water samples and archived at -20 °C. In conjunction with the phytoplankton sampling, corresponding water temperature and conductivity were measured using a CTD (conductivity, temperature, depth; model SBE 19plus V2, Sea-Bird Scientific, Bellevue, Washington, USA). Nutrient samples were collected monthly from the Homer, AK environmental monitoring station (59.4409 °N, 151.7209 °W) maintained by the Kachemak Bay National Estuarine Research Reserve (KBNERR; triangle, Fig. 1C). The nutrient sampling was independent of the water sampling. Nutrient measurement data for phosphate, ammonium, and nitrate+nitrite as well as water temperature and salinity for Kachemak Bay were obtained from the National Estuarine Research Reserve System Centralized Data Management Office website (http://cdmo.baruch.sc.edu/get/export.cfm). Homer, AK airport wind speed data (2012-2015)

were downloaded from NOAA's National Centers for Environmental Information website https://www.ncdc.noaa.gov/cdo-web/datasets/GHCND/stations/GHCND:USW00025507/detail. Precipitation data for Homer, AK was downloaded from The Alaska Climate Research Center's website http://climate.gi.alaska.edu/acis_data. A monthly average interannual stratification index (2012-2015) was calculated using CTD measurements of temperature and salinity obtained from the middle of Kachemak Bay at Transect 9, station 6 (Fig. 1C). The stratification index was calculated as the slope of the vertical density gradient from the surface to 30 m depth (Vandersea et al. 2018).

2.2 Satellite imagery processing

Satellite imagery of algal biomass was collected before, during, and after the *Karenia mikimotoi* bloom and was used to assess the geographical extent and relative magnitude of the bloom. The satellite imagery also corroborated qPCR cell abundance estimates for water samples collected from approximately the same time as the satellite images in lower Cook Inlet and Kachemak Bay. Imagery from the Moderate Resolution Imaging Spectroradiometer (MODIS) covering south-central Alaska were obtained from NASA Goddard Space Flight Center's Ocean Biology Processing Group (https://oceancolor.gsfc.nasa.gov). The Aqua level 0 granules were processed using the NOAA satellite automated system, which incorporates National Aeronautics and Space Administration's (NASA) standard ocean color satellite processing software distributed within the Sea-viewing Wide Field-of-view Sensor (SeaWiFS) Data Analysis System (SeaDAS) package (version 7.5 https://seadas.gsfc.nasa.gov/). Remote sensing reflectance (Rrs) and top-of-atmosphere reflectance corrected for molecular scattering (Rayleigh) and absorption (Rho_s) products were created for the visible and near infrared bands.

Near-infrared reflectance allows differentiation between chlorophyll and water. Chlorophyll reflects the near-infrared spectrum while near-infrared radiation is absorbed more by water. Products were mapped to an Albers Equal Area projection at 1100 m pixel resolution to produce level3 multi-band GeoTiffs. Multiple granules overlapping the area of interest from the same day were composited based on time of swath. The Red Band Difference (RBD) algorithm described in Amin et al. (2009) was applied using the processed Rho_s bands as

$$RBD = Rho\_s(678) - Rho\_s(667)$$

to highlight areas of high algal biomass.

2.3 Cell culturing

Cell cultures were used as a source of positive control DNA for the qPCR assays and to construct qPCR standard curves described below. Four *Karenia mikimotoi* strains (CC21, CC22, CCFW64, CCFW131) were obtained from Dr. Carmelo Tomas of University of North Carolina Wilmington, Center for Marine Science. The cultures were maintained using methods described in Hardison et al. (2013).

2.4 DNA extraction, sequencing protocols and molecular identification of Karenia mikimotoi

DNA extraction and PCR amplification of the *Karenia mikimotoi* SSU rDNA region was performed using reagents and methods adapted from Vandersea et al. (2012). Approximately 50 mL of Lugol's-preserved surface water was collected from Seldovia Bay, AK (Fig. 1C) during the *K. mikimotoi* bloom and concentrated by filtration onto a 47 mm, 8 µm pore size

polycarbonate filter (Whatman Nucleopore™, GE Healthcare Bio-sciences, Pittsburgh, Pennsylvania, USA). Genomic DNA was extracted from the filter using the Mo Bio Laboratories Power® Soil DNA Isolation Kit (Mo Bio Laboratories, Solana Beach, California, USA) following the manufacturer's protocol, except that 350 µL of cell lysate rather than the prescribed 450 µL was processed. Spectrophotometric analysis (260nm/280nm) of the DNA was conducted to assess DNA concentration and purity. An approximately 1750 bp product containing the SSU rDNA domain was PCR amplified using the GCG18SF (CACTTAGAGGAAGGAGAAGT) and G45R (ACGAACGATTTGCACGTCAG) primers. The PCR amplification reaction mixtures contained 20 mM Tris-HCl, pH 8.4, 3 mM $MgCl_2$, 50 mM KCl, 25 pmoles of each primer, 2.5 mM of each deoxynucleoside triphoshate, 0.2 units Platinum® *Taq* DNA polymerase (Invitrogen™ Life Technologies, Carlsbad, California, USA), and 10 ng of genomic DNA in a total reaction volume of 50 µL. An MJ Research MiniCycler® (MJ Research, Waltham, Massachusetts, USA) was used to conduct the PCR with the following cycling conditions: 2 min. at 95 °C, 35X (30 s denaturation at 95 °C, 30 s annealing temperature at 58 °C and an extension of 1.5 min at 72 °C), and a final 5 min extension at 72 °C. A 4 µL aliquot of each PCR reaction was checked for the presence of a specific amplification product by agarose gel electrophoresis (2% tris-acetate/EDTA, 100 V) and ethidium bromide staining.

The PCR product was purified using the Pure Link™ Quick PCR Purification Kit (Invitrogen Life Technologies). DNA templates were sequenced completely in both directions using the sequencing primers listed in Vandersea et al. (2012). The sequences were assembled using the Vector NTI Advance™ 11 program (Invitrogen Life Technologies) and aligned with related species to confirm the identity of the bloom. The GenBank accession numbers included in the SSU rDNA alignments were *Karenia selliformis* HM067007, *Karenia papilionacea*

HM067005, *Karenia brevis* FJ587219, DQ847434, EF492501, EF492502, EF492503 EF492504, AF274259, *Gymnodinium breve* AF172714, *Karenia mikimotoi* EF492505, FR865627, FJ587220, KU314866, MG022774, uncultured eukaryote HM581706, *Gyrodinium aureolum* AF172713, AJ415517, *Gymnodinium aureolum* DQ779991, AF172713, *Gymnodinium* cf. *mikimotoi* AF009216, *Gymnodinium mikimotoi* AF022195. The *Karenia mikimotoi* SSU rDNA gene sequence obtained in this study was deposited in GenBank (MH161392).

2.5 Design and testing of species-specific Karenia mikimotoi PCR primers

To identify species-specific *Karenia mikimotoi* PCR primer sites, *Karenia mikimotoi* ribosomal ITS rDNA sequences, obtained from GenBank, were aligned with corresponding ITS sequences from other related *Karenia* species using the ClustalX program (Thompson et al., 1997). Unique forward and reverse *K. mikimotoi* species-specific PCR primer sites were visually identified within the alignments. Each primer was subjected to a BLAST search using the National Center for Biotechnology Information (NCBI) BLAST tool to confirm specificity (Altschul et al., 1997). The primers were tested systematically for secondary PCR products using *K. mikimotoi* genomic DNA and the amplification conditions described below.

GenBank acession numbers used in the ITS rDNA sequence alignments: *Karenia mikimotoi* AF318223, AF318224, FJ823564, FR865627, HM807311- HM807314, HM807316-HM807319, HM807321, JF683413, JN595871, JN595872, *Karenia bidigitata* FJ823560, FJ823561, HM067003, HM807322, HM807323, *Karenia brevis* AF352823-AF352827, AF352368, AF352369, *Karenia papilionacea* AB623224, KJ508367, LC055192- LC055195, LC055202, LC055204, LC055206, LC055209, *Karenia selliformis* HM067008, HM807324, *Karenia umbella* FJ823566, MF781065-MF781068, *Karlodinium veneficum* EF036540,

AY245692, KU314867, KP639236, KT389958, *Karlodinium* sp. FN357291, *Karenia* sp. AM184206, *Karenia* sp. AF318225, *Gymnodinium* sp. Chile_53/16 AF318247, *Gymnodinium aureolum* DQ779991, KT390017, Uncultured eukaryote GU941834.

2.6 Environmental sample DNA extraction and qPCR assay

Molecular analyses of environmental samples were performed using reagents and methods described in Vandersea et al. (2018). DNA was extracted from the Lugol's-preserved phytoplankton samples collected during 2011-2017 and stored at -20 °C pending *Karenia mikimotoi* qPCR assay analysis. The *Karenia mikimotoi* qPCR assay was conducted using an Eppendorf Mastercycler® ep realplex 4 system with white Eppendorf real-time tube strips (Eppendorf North America, Inc., Westbury, New York, USA) and a total reaction volume of 10.5 µL per tube. Each PCR reaction mixture contained 4.5 µL of 5 Prime RealMasterMix SYBR ROX 2.5x [0.05 units μL^{-1} Taq DNA polymerase, 10 mM $Mg(CH_3COO)_2$, 1.0 mM dNTPs, 20X SYBR® Green solution], each primer at a concentration of 0.15 µM, 4.7 µL of sterile deionized water, and 1 µL of template DNA [*Karenia mikimotoi* forward primer (5'-TATTCTCTCATGCCACTGTCATCT-3') reverse primer (3'- CAATGCATCAGGGGCAGGA-5')]. Thermal cycling conditions included denaturation at 95°C for 2 min followed by 40 cycles at 95°C for 10 s, annealing for 15 s at 60°C with a subsequent extension at 68°C for 20 s to produce a 102 bp PCR product. A melting curve analysis was performed following thermal cycling to check the specificity of the PCR reactions. A limit of ±0.5°C for melting temperature peak shift was set as the cutoff for species-specific amplifications.

2.7 qPCR standard curves

Standard curves were constructed to calibrate the *Karenia mikimotoi* qPCR assay following methods described in Vandersea et al. (2017) using serially diluted PCR amplicons as well as dilutions of live, cultured *Karenia mikimotoi* cells. First, an rDNA fragment (3' SSU – 5' LSU) that contained the qPCR assay target sites was PCR amplified using the G45F forward and LSUB reverse primers and the cycling conditions described above. The DNA concentration of the purified amplicon was estimated spectrophotometrically by measuring UV absorbance at 260 nm. To construct standard curves, the purified amplicon was serially diluted 1:10 in dH_2O and encompassed six orders of magnitude. Each serial dilution was qPCR amplified for 40 cycles using the *K. mikimotoi* species-specific primers followed by a melting curve analysis to check for secondary qPCR products and primer dimers. The qPCR assay limit of detection (LOD) for the diluted PCR amplicon based standard curves was the lowest copy number concentration that yielded linear Cq values. For each curve, the Cq values generated from the tenfold serial dilutions were plotted against the log transformed copy numbers to obtain regression equations. Regression analyses were performed to calculate the slope values and confirm the linearity of the standard curves.

To construct cell based standard curves, four strains of *Karenia mikimotoi* cultures in log phase growth were gently mixed to ensure homogenization and then cell concentrations were measured in triplicate using a Beckman Coulter Multisizer™ 3 fitted with a 280 µm aperture tube (Beckman Coulter Inc., Brea, CA, USA). Individual cell dilutions ranging from 350 to 3.32 x 10^5 cells were prepared in triplicate using sterile filtered seawater at a salinity of 25. For each replicate sample, 100 mL of cells were concentrated by filtration onto 47 mm, 8 µm pore size polycarbonate filters as described above. Genomic DNA extraction and qPCR amplification were performed as described above. Each assay incorporated 1 µL of the 50 µL DNA extract in

the qPCR reaction mix. Standard curves were constructed by plotting the triplicate Cq values against the log transformed cell concentrations. A regression analysis of the Cq vs. log transformed cell concentrations was performed to calculate the slope values and confirm the linearity of the standard curves. The qPCR assay limit of detection for the cell based standard curves was the lowest cell concentration, ranging over three orders of magnitude, that amplified and yielded linear Cq values.

2.8 Estimating cell numbers

Methods described in Vandersea et al. (2017) were used to calculate *Karenia mikimotoi* cell number estimates from DNA extracted from environmental samples collected in lower Cook Inlet and Kachemak Bay. First, the number of extractable PCR amplicons per environmental sample was calculated by solving the regression equations derived from diluted PCR amplicon-based standard curves using Cq values acquired from qPCR assay of environmental samples. This value was divided by the number of *K. mikimotoi* extractable rDNA copies per cell that was estimated from the regression equations for the cell based standard curves. The sample volume (10 – 40 L) and the volume removed from the collection bottle of the phytoplankton net (100 mL) were used to calculate the number of cells per liter in each sample and abundance was expressed as *K. mikimotoi* cell equivalents per liter of seawater (cell eq. L^{-1}).

2.9 qPCR assay controls

To assess potential DNA contamination and PCR inhibitors in the extracted field samples, each qPCR assay included a positive control, a negative DNA control, a blank extraction control, and two spiked DNA controls. The positive control contained a known

amount of target DNA in the qPCR reaction mixture and ensured that the qPCR reagents were properly assembled. The negative control included the addition of 1µL of reaction buffer to a subset of reaction mixes in order to test for contaminated reagents or cross-contamination between samples. The blank controls were incorporated during the DNA extractions of the environmental samples to test for potential DNA contamination during the extraction process. Spiked DNA controls consisted of adding target DNA to a subset of the environmental samples to determine if PCR inhibitors were present.

2.10 Literature survey

Two literature surveys were performed. The objective of the first survey was to assemble a representative table of *Karenia mikimotoi* bloom conditions for comparison with the Kachemak Bay bloom. The table included cell densities, prevailing temperatures, salinities, and other factors that favored blooms. It also included temperature ranges and salinities over which blooms were observed. The second survey was conducted to examine the relationship between temperature and *K. mikimotoi* growth, including both laboratory and field estimates. The bloom in this study occurred at unusually low temperatures and it was of interest to estimate to what extent *in situ* growth accounted for the observed cell densities versus hydrodynamic accumulation. Growth rates were calculated using $\mu = \ln\left(\frac{Nf}{Ni}\right)/T$, where Ni and Nf are the initial and final qPCR cell estimate concentrations and T is the incubation time (Nakamura et al. 1995).

3. Results

Light microscopy observation of the Kachemak Bay bloom species revealed an unknown Gymnodinoid dinoflagellate (Fig. 2). Molecular characterization of the SSU rRNA gene confirmed the species as *Karenia mikimotoi* and established a new dinoflagellate observational record for Kachemak Bay, AK. Based on these findings, a quantitative PCR assay was developed to assess abundance and distribution of *K. mikimotoi* in relation to environmental observations in lower Cook Inlet. The assay targeted the ITS2 rDNA of the ribosomal gene complex. The assay sensitivity and LOD was tested using cell concentrations ranging from 10 to 3.32 x 10^5 cells diluted in 100 mL of filtered seawater. The assay was capable of detecting as few as10 cells, however the Cq values were variable and couldn't be included as members of linear standard curves. The assays' quantitative LOD was therefore 350 cells in 100 mL of filtered seawater and exhibited a linear range up to 3.32 x 10^5 cells. A dilution series of a PCR amplicon that contained the *K. mikimotoi* target sequence was also used to test the sensitivity of the assay. The LOD of the diluted PCR amplicon was ~430 copies and the assay was linear over six orders of magnitude. Standard curves were constructed using 10-fold serial dilutions of purified PCR amplicons as well as DNA extracted from known concentrations of live *K. mikimotoi* cells. The slope values of the diluted PCR amplicon curves typically varied between -3.21 and -3.32 with corresponding amplification efficiencies ranging from 99 – 104%. The cell based standard curves were linear over three orders of magnitude with slope values that ranged between -3.24 and -3.33 and possessed amplification efficiencies ranging from 99 – 103%. The differences in the slope values of the cell based standard curves and the diluted PCR amplicon standard curves was compared and varied by less than 0.1. The linear relationships and representative data from typical standard curves that were used to calculate the regressions are

shown (Fig. 3). The empirical relationship between extractable rDNA copy numbers and cell numbers for *K. mikimotoi* was calculated to be approximately four extractable copies per cell.

3.1 Temperature, salinity, stratification, and Karenia mikimotoi *bloom development in Kachemak Bay and Lower Cook Inlet*

A time series analysis of water temperature, salinity, stratification, and abundance of *Karenia mikimotoi* in Kachemak Bay and lower Cook Inlet from 2012-2015 is shown in Figure 4. Phytoplankton samples and physical data were collected along Transects 3, 4, 6, 7 & 9, and from Jakolof Bay dock, Kasitsna Bay dock, and Seldovia Bay (Figs. 1B and 1C). For Kachemak Bay, the analysis revealed that water temperatures reached annual minima (~ 2 – 4 ˚C) during February-April while salinities reached annual maxima during April (31 – 32.2). Salinity decreased in May-June (26.5–31.5) as water temperatures increased, indicating input of snow melt to the Bay. Water temperatures reached annual maxima during July-September (12.6 - 14 °C) while salinities varied between 21 - 32. The first presence of *Karenia mikimotoi* was detected in a water sample collected at the Kasitsna Bay, NOAA Laboratory dock by qPCR on 22 July 2013, and at a concentration of ~ 30 cell eq. L^{-1} (Fig. 4D). The first bloom concentrations (> 10^3 cells eq. L^{-1}) were detected 30 August 2013, at the Kasitsna Bay dock and at Transect 9, station 1 (~1.2 x 10^3 – 7.9 x 10^5 cell eq. L^{-1}). Water temperatures during August ranged from 9 – 12 °C and salinities varied between 24.8 – 31.8. During September, water temperatures started decreasing and ranged from 8 – 11.8 °C while salinities varied from 24.8 – 31.4. Maximum *K. mikimotoi* cell number estimates detected in October were less than September and ranged from 7.4 x 10^2 – 3.0 x 10^5 cell eq. L^{-1}. From November, 2013 to March, 2014 water temperatures continued to decline (8.8 – 3.26 °C) while salinities increased (25.8 –

32.1) due to onset of winter conditions and reduced freshwater input. *K. mikimotoi* bloom concentrations were detected in five samples during this period with cell concentrations ranging from 7.4 x 10^2 – 5.9 x 10^4 cell eq. L^{-1}. The last sample to contain measurable cell concentrations was collected at Transect 4, station 2 on 11 April 2014 and contained ~3.5 cell eq. L^{-1}. In lower Cook Inlet, *K. mikimotoi* was detected along Transects 3 and 6 during November 6 - 8, 2013 (Figs. 1B and 4G). Cell concentrations at these stations ranges from 2.9 x 10^2 – 1.84 x 10^4 cell eq. L^{-1}.

The seasonal cycle of stratification and mixing of the upper water column during 2013 was compared to *K. mikimotoi* qPCR cell estimates for water samples collected during the course of the bloom (Figs. 4C and 4D). The stratification index in this region of Kachemak Bay indicated more stable water column conditions (≥ 0.1) during June – August (0.1 – 0.3), and mixed conditions (≤ 0.1) from September through May of 2014 (Fig. 4C).

3.2 Precipitation, wind speeds, and Karenia mikimotoi *bloom development*

Average daily precipitation and wind speed data for Homer, AK from 2012 - 2015 were plotted in relation to *Karenia mikimotoi* qPCR cell estimates to investigate any correlation between rainfall, wind speeds, and the bloom cycle (Fig. 5). The total amount of rainfall that occurred in Homer during May - September of 2013, leading up to the *K. mikimotoi* bloom, was ~324 mm (Fig. 5A). Average daily wind speeds before and during bloom development (May – September) were < 6 m/s (Fig. 5B).

3.3 Seasonal nutrient cycling in comparison to bloom development

Nutrient data collected from the Homer Spit monitoring station during 2012 - 2015 are shown in relation to *Karenia mikimotoi* qPCR cell abundance estimates in Figure 6. The data revealed that both surface and subsurface nitrate + nitrite concentrations (NO_2^- + NO_3^-) began declining from winter time maxima (>0.2mg L^{-1}) in April - May to summertime minima (<0.05 mg L^{-1}) in June – August, and then began increasing in autumn (September – November, Fig. 6A). Dissolved surface and subsurface phosphate (PO_4^{3-}) exhibited a similar pattern with concentrations of 0.03 - 0.04 mg L^{-1} in winter that declined to 0.01 - 0.025 mg L^{-1} during the summer (Fig. 6B). Both surface and subsurface NO_2^- + NO_3^- and PO_4^{3-} levels exhibited similar seasonal patterns, indicative of nutrient drawdown during the April - June phytoplankton bloom each year. Surface concentrations of ammonium (NH_4^+) were generally at their highest from October - March (0.03-0.05 mg L^{-1}) and decreased to ≤ 0.02 mg L^{-1} during June - August (Fig. 6C). Near bottom NH_4^+concentrations were similar to surface levels in the winter months, but then increased sharply during May-September (0.03 - 0.08 mg L^{-1}, Fig. 6C).

3.4 Literature survey

The first literature survey revealed *Karenia mikimotoi* bloom concentrations typically ranged from several hundred thousand cells L^{-1} to around 10,000,000 cells L^{-1} with as many as 69,000,000 cells L^{-1} reported (Table 1). Blooms were reported occurring between 12 and 31.2 °C and at salinities between 6 and 35.7. Live cells were observed between 4 and 31.2 °C and at salinities between 0 and 35.8. Other factors common to bloom formation included water column stability, a ready source of nutrients, relatively calm conditions, and favorable hydrodynamic conditions. Water column stability was typically the result of runoff setting up a stable pycnocline, increased temperatures establishing a thermocline, or both. The exception was

shallow systems (~10-15m), such as estuaries where blooms served the same function as a pycnocline or thermocline. Nutrients were either input directly through runoff or other processes or were accessible from a nutrient rich layer below the thermocline or pycnocline by diel vertical migration. Upwelling zones and high wind driven mixing were not conducive to bloom formation.

The results of the growth rate literature survey are shown (Fig. 7). A majority of the laboratory studies revealed that *Karenia mikimotoi* growth increased from 15 to 27 °C reaching a maximal growth rate between 0.3 and 0.63 d^{-1} (Fig. 7A). The primary exception was the study by Gentien et al. 2007 where growth rates increased from 0 at 12 °C to a maximum of 0.63 d^{-1} at 17 °C (black diamond symbols, Fig. 7A). In contrast, a majority of growth rate estimates from field studies at water temperatures between 13 and 30 °C ranged from 0.3 to 0.44 d^{-1} (Fig. 7B). The one exception was a growth rate of 0.9 estimated by Chang and Carpenter (1985), which is likely an overestimate caused by bioaccumulation due to hydrodynamics or diel vertical migration (Shikata et al., 2015; Sourisseau et al., 2016). The growth rates calculated in the current study were consistent with growth versus temperature data from other studies (star symbols, Fig. 7B). They also spanned a lower temperature range not previously recorded. The data indicated that growth ceased around 8 ^{o}C. The negative values represent the period of rapid decline in the bloom as water temperatures declined.

3.5 Satellite imagery

Satellite imagery from the Moderate Resolution Imaging Spectroradiometer (MODIS) covering south-central Alaska for 2013 was obtained from NASA Goddard Space Flight Center's Ocean Biology Processing Group and was used to assess the geographical extent and relative magnitude

of the bloom (Fig 8). The satellite imagery provided a visual record of the bloom progression and was also used to corroborate qPCR cell abundance estimates for water samples collected from approximately the same time as the satellite images in lower Cook Inlet and Kachemak Bay.

4. Discussion

This is the first record of a *Karenia mikmotoi* bloom in Alaska. qPCR assay analyses of DNA samples collected as part of a long-term study of *Alexandrium catenalla* in Kachemak Bay and lower Cook Inlet Alaska revealed the earliest evidence of the bloom occurred in late July, 2013 and lasted through April, 2014 (Fig. 4D). Maximum bloom concentrations were detected in late September even though water temperatures peaked during July (12-14 °C) and decreased during August and September (12-8 °C) as the bloom was maturing (compare Figs 4A and 4D). These data suggest that after initial phases of the bloom, water temperature was not the primary factor controlling subsequent bloom development. Similar *K. mikimotoi* bloom intensification after annual water temperatures have peaked has been observed in Scottland (Davidson et al. 2009) and in Japan (Honjo, 1994). Furthermore, analysis of salinity and stratification in relation to *K. mikimotoi* abundances in Kachemak Bay showed that the timing of bloom development coincided with salinity minima as well as maximum water column stratification (Figs 4B-4D). During summer, snow melt has a more pronounced impact on salinity and vertical structure of the water column in Kachemak Bay than runoff from rainfall (Abookire et al., 2000; Okkonen et al., 2009). However, precipitation measurements from Homer showed that 70% of the annual rainfall in 2013 occurred during August and September, with a total of 227 mm during this period. This was above average rainfall for late summer and likely augmented the snow melt

runoff into the Bay, increasing freshwater impact on vertical water column structure. Salinities during this period ranged from 24.8 – 31.8 (Fig. 3B), well within the salinity tolerances of *K. mikimotoi* that have been reported previously (Gentien, 1998; Kimura et al., 1999; Aoki et al., 2017; Table 1). Wind speeds leading up to the bloom were relatively light and were measured at < 6 m s^{-1} (Fig 5). Nutrient analyses of surface and bottom $NO_2^- + NO_3^-$, PO_4^{3-}, and NH_4^+ revealed seasonal patterns indicative of nutrient drawdown at the surface during the April-June phytoplankton bloom (Fig. 6). Minimum concentrations of surface and bottom $NO_2^- + NO_3^-$ occurred during the summer and increased in autumn (Fig. 6A). In contrast, surface PO_4^{3-} and NH_4^+ measurements revealed they were at their lowest during summer while near bottom concentrations were more elevated and well within ranges reported to support *K. mikimotoi* blooms in other field studies (DIN 0.23-18.5 umol L^{-1}; PO_4^{-3} 0.03-2.42 umol L^{-1} fromYamaguchi and Itakura, 1999; Li et al., 2009) (Fig. 6B).

In summary, these physical data indicated that a very stable, stratified, water column existed in the Bay during the summer months of 2013 with pools of PO_4^{3-} and NH_4^+ existing at depth during the early stages of bloom formation. *K. mikimotoi*'s ability to vertically migrate would have allowed the cells access to deep nutrient pools, likely providing a competitive advantage over other phytoplankton species (Koizumi et al., 1996; Nakamura et al., 1996; Kimura et al., 1999; Aoki et al., 2017). Review of the literature revealed that water column stratification and high nutrients are consistent factors associated with *K. mikimotoi* blooms (Table 1). These conditions also correspond with environmental conditions promoting bloom formations of other dinoflagellate species in many coastal systems (Margalef, 1975; Smayda, 1980; Sournia, 1982; Chang and J. Carpenter, 1985; Paerl, 1988; Daniel et al., 1992; Widdicombe et al., 2010; Hartman et al., 2014; Barnes et al., 2015). Moreover, as the *K.*

mikimotoi bloom developed during August-September, surface PO_4^{3-} and NH_4^+ concentrations increased (Figs 6B and 6C). The increased availability of these nutrients would have further supported bloom development and help to explain the high concentrations of cells that were detected at the peak of the bloom (Fig. 4D, 10^7 cells L^{-1}).

The bloom concentrations measured in this study were among the highest that have been reported (Table 1). This leads to the logical question of whether the bloom concentrations were the result of *in situ* growth or hydrodynamic accumulation? A literature review revealed that maximal growth of *Karenia mikimotoi* (0.62 to 0.69 d^{-1}) in laboratory studies, occurred between 15 to 26 °C, depending on the strain (Fig. 7A). In these studies, growth never exceeded one division per day (0.69 d^{-1}) and markedly declined below 12-15 °C. The estimated field growth rates calculated in our study were 0.29 and 0.13 d^{-1} in August and September when average monthly water temperatures were 11.3 and 10.4 °C respectively (star symbols, Fig. 7B). Growth rates were almost zero or negative as water temperatures declined below 8 °C (Fig. 7B). These growth rates agreed with previous laboratory and field studies that reported comparable water temperatures and were sufficiently high that *in situ* growth alone could account for development of the bloom given the standing stock of cells present in August (Fig. 4D). Development of *K. mikmotoi* blooms over similar time periods have been observed in other systems, though usually at higher water temperatures (Lindahl et al., 1983; Chang and Carpenter, 1985; Honjo, 1994; Blasco et al., 1996; Davidson et al., 2009).

MODIS-Aqua satellite imagery of south-central Alaska from 2013 provided a visual record of the bloom progression and the bloom's extent (Fig. 8). Despite cloud cover in the region that obscured the majority of the daily satellite images, a relative fluorescence image from 24 August demonstrated that LCI and Kachemak Bay exhibited very low algal biomass (Fig. 8).

Similarly, qPCR cell estimates from a water sample collected from the Kasistna Bay Dock on 23 August confirmed low *Karenia mikimotoi* concentrations (< 10 cells L^{-1}). Satellite imagery collected 1 October documented that the bloom covered most of Kachemak Bay and confirmed high biomass associated with peak bloom phase (Figs. 4D and 8). Bloom concentrations in Kachemak Bay began declining in October through November as water temperatures were cooling (Figs. 4 and 8). Previous studies have implicated wind events, increased mixing, autotoxicity, light limitation, and grazing as factors that can cause *K. mikimotoi* blooms to decline (Nakamura et al., 1996; Gentien et al., 2007; Barnes et al., 2015). Analysis of water column stability revealed that water column stratification was breaking down during the period that the *K. mikimotoi* bloom was declining (arrowhead, Fig. 4C). Grazing is less likely of a factor because zooplankton populations in the region decline significantly in the late fall and winter (McKinstry and Campbell, 2018). Although other factors may have prompted the bloom to decline, water column mixing and cooling water temperatures appear to have been potential drivers.

Satellite imagery from 23 October and 12 November showed a decline in algal biomass in Kachemak Bay (Fig 8). Interestingly, in the image from 23 October, a high algal biomass signature is present in the Shelikof Strait on the west side of Kodiak Island. This region of Kodiak Island is sparsely populated and there were no reports of an algal bloom. Unfortunately satellite imagery between 1 and 23 October was obscured by cloud cover that prevented monitoring of potential bloom transport. Therefore it is unknown if the bloom was transported to Shelikof Strait. Salinities in Kachemak Bay during this period ranged from 23.7 to 31.3 (Fig. 4B), well within the salinity tolerances of *Karenia mikimotoi* that were reported previously (Gentien, 1998; Kimura et al., 1999; Aoki et al., 2017; Table 1). Nutrient concentrations (Fig. 6)

were also within ranges reported to support *K. mikimotoi* blooms in other field studies (DIN 0.23-18.5 umol L^{-1}; PO_4^{-3} 0.03-2.42 umol L^{-1} fromYamaguchi and Itakura, 1999; Li et al., 2009). In early December and again in early January, two bloom concentrations were detected in samples containing $4.5x10^4$ and $5.9 x10^4$ cells eq. L^{-1}. The significance of this is that water temperatures between December and January averaged ~5 °C. Previously, Blasco et al., (1996) reported 4 ºC as the lowest temperature where live cells had been observed (Table 1) and Shimada et al. (2016) reported *K. mikimotoi* in Hakodate Bay, Japan at 9 °C. Other corresponding laboratory and field studies indicated that *K. mikimotoi* growth ceases below 10 °C (Fig. 7). In contrast, estimated *K. mikimotoi* field growth rates from our study showed active growth between 10-12 °C, with growth ceasing below ~8 °C. This suggests that the bloom concentrations observed in December and thereafter were residual populations from the fall bloom that were no longer actively growing. The last qPCR positive sample from Kachemak Bay was detected in early April 2014 and contained < 10 cells eq. L^{-1}. These data indicated some *K. mikimotoi* cells were able to endure relatively cold water temperatures, but succumbed as water temperatures from January to April 2014 continued to decline and ranged between 3.0 to 5.5 °C.

Another important, but unanswered question is what led to the establishment of the initial cell population in July 2013? The conditions present in Kachemak Bay during 2013 were not significantly different from preceding years (Vandersea et al. 2018), yet the bloom occurred during 2013. In a review of harmful algal bloom dispersal, Smayda (2007) described enigmatic and exotic blooms as “usually precipitous, abundant, ephemeral, often recorded as ‘first events’, and the source of the propagules seeding the bloom is usually unknown”. The *Karenia mikimotoi* bloom in Kachemak Bay certainly qualified as an exotic bloom. One possible

explanation for the introduction of the *K. mikimotoi* seed population was through discharge of ballast water. Cook Inlet is a highly trafficked waterway, supporting the majority of the state's population as the only sea-route to the Port of Anchorage. Commercial vessels would have regularly entered Kachemak Bay during 2013 providing opportunities for a ballast water introduction of *K. mikimotoi*. However, given the similarity in prevailing environmental conditions during previous years, coupled with the lack of *K. mikimotoi* blooms, it is unlikely this is was the mechanism leading to the establishment of the intial *K. mikimotoi* population.

A more likely hypothesis, is a long distance, latitudinal dispersion of *K. mikimotoi* from Japan. In March of 2011, a massive tsunami struck the east coast of Japan and swept an estimated five million tons of debris out to sea (Ministry of the Environment, Japan, 2012). The circulation patterns of the North Pacific and Gulf of Alaska are favorable for transport and dispersal of tsunami debris along southeast and south central Alaskan shorelines in the Gulf of Alaska. Marine debris from this event started arriving to North American shorelines in 2012, including beaches in Alaska adjacent to Kachemak Bay (Carlton et al., 2017; Murray et al., 2018; ADEC, 2019). We speculate that *K. mikimotoi* cells could have rafted into lower Cook Inlet and Kachemak Bay or were entrained in a water mass carrying marine debris originating from Japan. Support for this hypothesis comes from Carlton et al. (2017) who documented 289 living Japanese coastal marine species that landed with tsunami debris on coastlines from Midway Atoll to Hawaii Island and from south central Alaska to California. Further, the potential for dinoflagellate dispersal by drift algae or plastic debris also has been noted by others (Bomber et al. 1988; Faust and Gulledge, 1996; Masó et al 2003). The long transit time across the Pacific would have provided an extended acclimatization period for *K. mikimotoi* and may help explain why the bloom persisted in Kachemak Bay at some of the lowest recorded water

temperatures for *K. mikimotoi*. The life cycle for *K. mikimotoi* is not fully described. It is possible that cyst stages may have overwintered in Kachemak Bay (Liu et al. 2018). However, continued qPCR assay of water samples collected from Kachemak Bay and lower Cook Inlet from 2011-2016 have all been negative (Fig. S1), suggesting that the *K. mikimotoi* bloom of 2013 in Kachemak Bay was a singular event and the cells have not become established permanently as a common component of the local phytoplankton assemblage.

Acknowledgements

Special thanks are given to NOAA's Hollings Undergraduate Scholarship Program and Phytoplankton Monitoring Network, the captains and crews of the RV Edgecombe and RV Barnacle, the Seldovia Village Tribe, and the Jakolof Bay Oyster Company for assistance with data collection and project planning. We thank Dr. Carmelo Tomas for sharing cultures of *Karenia mikimotoi* that were used as positive controls. We also thank the two anonymous reviewers whose comments helped to improve the manuscript. Funding for this project was provided by NOAA′s National Centers for Coastal Ocean Science (NCCOS) through the Kachemak Bay Habitat Focus Area initiative and North Pacific Research Board Project 1118. Pursuant to NOAA Administrative Special Award Condition #16 and ERD Special Award Condition #4, manuscripts resulting from this NOAA/OCRM-supported research and data collection effort that are produced for publication in open literature, including refereed scientific journals, shall acknowledge that the research was conducted under an award from the Estuarine Reserves Division, Office of Ocean and Coastal Resource Management, National Oceanic and Atmospheric Administration.[CG]

References

Abookire, A.A., Piatt, J.F., Robards, M.D., 2000. Nearshore Fish Distributions in an Alaskan Estuary in Relation to Stratification, Temperature and Salinity. Estuar Coast Shelf Sci 51, 45-59.

ADEC, 2019. Alaska Department of Environmental Conservation. Tsunami and marine debris in alaska. Available at https://dec.alaska.gov/eh/marine-debris/ (7 October 2019).

Al-Kandari, M.A., Highfield, A.C., Hall, M.J., Hayes, P., Schroeder, D.C., 2011. Molecular tools separate harmful algal bloom species, *Karenia mikimotoi*, from different geographical regions into distinct sub-groups. Harmful Algae 10, 636-643.

Altschul, S.F., Madden, T.L., Schäffer, A.A., Zhang, J., Zhang, Z., Miller, W., Lipman, D.J., 1997. Gapped BLAST and PSI-BLAST: a new generation of protein database search programs. Nucleic Acids Res 25, 3389-3402.

Anchorage Daily News, 2016. Armstrong, M., Turning tsunami trash from Alaska coast into Kachemak Bay art. Available at: https://www.adn.com/alaska-news/article/turning-tsunami-trash-alaska-coast-kachemak-bay-art/2012/08/25/ (7 October 2019).

Aoki, K., Kameda, T., Yamatogi, T., Ishida, N., Hirae, S., Kawaguchi, M., Syutou, T., 2017. Spatio-temporal variations in bloom of the red-tide dinoflagellate *Karenia mikimotoi* in Imari Bay, Japan, in 2014: Factors controlling horizontal and vertical distribution. Mar Pollut Bull 124, 130-138.

Aokia, K., Kuroda, H., Setou, T., Okazaki, Yamatogi, M., T. Hirae, S., Ishida, N., Yoshida, K., Mitoya, Y., 2019. Exceptional red-tide of fish-killing dinoflagellate *Karenia mikimotoi* promoted by typhoon-induced upwelling. Estuar Coast Mar Sci 219, 14-23.

Auinger, M.B., Pfandl, K., Boenigk, J., 2008. Improved methodology for identification of protists and microalgae from plankton samples preserved in Lugol's iodine solution: Combining microcopic analysis with single-cell PCR. Appl Environ Microbio 74, 2505-2510.

Barnes, M.K., Tilstone, G.H., Smyth, T.J., Widdicombe, C.E., Gloël, J., Robinson, C., Kaiser, J., Suggett, D.J., 2015. Drivers and effects of *Karenia mikimotoi* blooms in the western English Channel. Prog Oceanogr 137, 456-469.

Blasco, D., Bérard-Therriault, L., Levasseur, M., Vrieling, E.G., 1996. Temporal and spatial distribution of the ichthyotoxic dinoflagellate *Gyrodinium aureolum* Hulburt in the St Lawrence, Canada. J Plankton Res 18, 1917-1930.

Bomber, J.W., Morton, S.L., Babinachak, J.A., Norris, D.R., Morton, J.G., 1988. Epiphytic dinoflagellates of drift algae another toxigenic community in the ciguatera food chain. Bull Mar Sci 18, 204-214.

Carlton, J.T., Chapman, J.W., Geller, J.B., Miller, J.A., Carlton, D.A., McCuller, M.I., Treneman, N.C., Steves, B.P., Ruiz, G.M., 2017. Tsunami-driven rafting: Transoceanic species dispersal and implications for marine biogeography. Science 357, 1402-1406.

Chang, F.H., 1996. A review of knowledge of a group of closely related, economically important toxic *Gymnodinium*/*Gyrodinium* (Dinophyceae) species in New Zealand. J Roy Soc New Zeal 26, 381-394.

Chang, J., Carpenter, E.J., 1985. Blooms of the dinoflagellate *Gyrodinium aureolum* in a Long Island Estuary: box model of bloom maintenance. Mar Biol 89, 83–93.

Dahl, E., Brockmann, U.H., 1985. The growth of *Gyrodinium aureolum* Hulburt in in situ experimental bags. In: Anderson, D. M., White, A.W. ,Baden, D.G. [Eds.], Toxic Dinoflagellates. Elsevier, New York, pp. 233–238.

Dahl, E., Tangen, K., 1993. 25 Years experience with *Gyrodinium aureolum* in Norwegian waters. In: Smayda, T.J., Shimizu, Y. (Eds.), Toxic Phytoplankton Blooms in the Sea. New York, Elsevier, pp. 15-22.

Dai, A.-Q., Shi, X.-Y., Ding, Y.-Y., Tang, H.-J., Wang, L.-S., Wang, X.-L., 2014. Effects Of temperature on the growth and nitrate reductase activity of *Chaetoceros curvisetus* and *Karenia mikimotoi*. Prog. Biochem. Biophys. 41, 896-903.

Daniel, D., Herbland, A., Maestrini, S.Y., 1992. Environmental conditions which lead to increase in cell density of the toxic dinoflagellates *Dinophysis* spp. in nutrient-rich and nutrient-poor waters of the French Atlantic coast. Mar Ecol Prog Ser 89, 53-61.

Davidson, K., Miller, P., Wilding, T.A., Shutler, J., Bresnan, E., Kennington, K., Swan, S., 2009. A large and prolonged bloom of *Karenia mikimotoi* in Scottish waters in 2006. Harmful Algae 8, 349-361.

Eckford-Soper, L.K., Daugbjerg, N., 2015. Development of a multiplex real-time qPCR assay for simultaneous enumeration of up to four marine toxic bloom-forming microalgal species. Harmful Algae 48, 37-43.

Engesmo, A., Strand, D., Gran-Stadniczenko, S., Edvardsen, B., Medlin, L.K., Eikrem, W., 2018. Development of a qPCR assay to detect and quantify ichthyotoxic flagellates along the Norwegian coast, and the first Norwegian record of *Fibrocapsa japonica* (Raphidophyceae). Harmful Algae 75, 105-117.

Faust, M.A., Gulledge, R.A., 1996. Associations of microalgae and meiofauna in floating detritrus at a mangrove island, Twin Cays, Belize. J Exp Mar Bio Ecol197, 159-175.

Garcia, V.M.T., Purdie, D.A., 1992. The influence of irradiance on growth, photosynthesis and respiration of *Gyrodinium* cf. *aureolum*. J Plankton Res 14, 1251-1265.

Gentien, P., 1998. Bloom dynamics and ecophysiology of the *Gymnodinium mikimotoi* species complex, In: Anderson, D.M., Cembella, A.D., Hallegraeff, G.M. (Eds.), Physiological Ecology of Harmful Algal Blooms. Springer-Verlag, Berlin, pp. 155-173.

Gentien, P., Lunven, M., Lazure, P., Youenou, A., Crassous, M.P., 2007. Motility and autotoxicity in *Karenia mikimotoi* (Dinophyceae). Phil Trans R Soc B 362, 1937–1946.

Hansen, G., Daugbjerg, N., Henriksen, P., 2000. Comparative study of *Gymnodinium mikimotoi* and *Gymnodinium aureolum*, comb. nov (= *Gyrodinium aureolum*) based on morphology, pigment composition, and molecular data. J Phycol 36, 394-410.

Hardison, D.R., Sunda, W.G., Shea, D., Litaker, R.W., 2013. Increased Toxicity of *Karenia brevis* during Phosphate Limited Growth: Ecological and Evolutionary Implications. PLoS One 8, e58545.

Hartman, S.E., Hartman, M.C., Hydes, D.J., Smythe-Wright, D., Gohin, F., Lazure, P., 2014. The role of hydrographic parameters, measured from a ship of opportunity, in bloom formation of *Karenia mikimotoi* in the English Channel. J Mar Syst 140, 39-49.

Holligan, P.M, Harris, R.P., Newell, R.C., Harbour, D.S., Head, R.N., Linley, E.A.S., Lucas, M.I. Tranter, P.R.G., Weekley, C.M., 1984. The vertical distribution and partitioning of organic carbon in mixed, frontal and stratified waters of the English Channel. Mar Ecol Prog Ser 14, 111-127.

Honjo, T., 1994. The biology and prediction of representative red tides associated with fish kills. Japan Rev Fish Sci 2, 225-253.

Honjo, T., Yamaguchi, M., Nakamura, O., Yamamoto, S., Ouchi, A., Ohwada, K., 1991. A relationship between winter water temperature and the timing of summer *Gymnodinium nagasakiense* red tides in Gokasho Bay. Nippon Suisan Gakk 57, 1679–1682.

Hu, S., Zhou, B., Wang, Y., Wang, Y., Zhang, X., Zhao, Y., Zhao, X., Tang, X., 2017. Effect of CO_2-induced seawater acidification on growth, photosynthesis and inorganic carbon acquisition of the harmful bloom-forming marine microalga, *Karenia mikimotoi*. PLoS One 12, e0183289.

Iizuka, S., 1979. Maximum growth rate of natural population of a *Gymnodinium* red tide. In: Taylor, D.L., Seliger, H.H. (Eds.), Toxic dinoflagellate blooms. Elsevier/North-Holland, New York, pp. 111-114.

Ishimaru, T., T. Takeuchi, Y. Fukuyo and M. Kodama (1989): The selenium requirement of *Gymnodinium nagasakiense*. In: Okaichi, T., Anderson, D.M., Nemoto, T. (Eds.), Red Tides: Biology, Environmental Science and Toxicology, Elsevier, Amsterdam. pp. 357-360.

Iyer, C.S.P., Robin, R.S., Sreekala, M.S., Kumar S.S., 2008. *Karenia mikimotoi* bloom in Arabian Sea. Harmful Algal News 37, 9-10.

Jeong, H.J., Yoo, Y.D., Kang, N.S., Rho, J.R., Seong, K.A., Park, J.W., Nam, G.S., Yih, W., 2010. Ecology of *Gymnodinium aureolum*. I. Feeding in western Korean waters. Aquat Microb Ecol 59, 239-255.

Jiménez, C., Niell, F., Figueras, F., Clavero, V., Algarra, P., Buela, J., 1992. Green mass aggregations of *Gyrodinium cf aureolum* Hulburt in the Ria of Pontevedra (North-West Spain). J Plankton Res 14, 705-720.

Jordan, M.B., Joint, I.R., 1984. Studies on phytoplankton distribution and primary production in the western English Channel in 1980 and 1981. Estuar Coast Shelf Sci 3, 25-34.

Kimura, B., Kamizono, M., Etoh, T., Koizumi, Y., Murakami, M., Honjo, T., 1999. Population development of the red tide dinoflagellate *Gymnodinium mikimotoi* in inshore waters of Japan. Plankton Biol Ecol 46, 37-47.

Koizumi, Y., Uchida, T., Honjo, T., 1996. Diurnal vertical migration of *Gymnodinium mikimotoi* during a red tide in Hoketsu Bay, Japan. J Plankton Res 18, 289-294.

Kok, J.W.K., Leong, S.C.Y., 2019. Nutrient conditions and the occurrence of a *Karenia mikimotoi* (Kareniaceae) bloom within East Johor Straits, Singapore. Reg Stud Mar Sci 27, March 2019, 100514.

Kong, F., Xu, Z., Yu, R., Yuan, Y., Zhou, M., 2016. Bloom dynamics and ecophysiology of the *Gymnodinium mikimotoi* species complex. Chin J Oceanol Limn 34, 902-914.

Le Corre, P., L'Helguen, S., Wafar, M., 1993. Nitrogen-source for uptake by *Gyrodinium* cf *aureolum* in a tidal front. Limnol Oceanogr 38, 446-451.

Lemley, D.A., Adams, J.B., Rishworth, G.M., 2018. Unwinding a Tangled Web: a Fine-Scale Approach towards Understanding the Drivers of Harmful Algal Bloom Species in a Eutrophic South African Estuary. Estuar Coasts 41: 1356.

Li, J., Glibert, P.M., Zhou, M., Lu, S., Lu, D., 2009. Relationships between nitrogen and phosphorus forms and ratios and the development of dinoflagellate blooms in the East China Sea. Mar Ecol Prog Ser 383, 11-26.

Lin, J.N., Song, J.J., Yan, T., Zhang, Q.C., Zhou, M.J., 2015. Large-scale dinoflagellate bloom species *Prorocentrum donghaiense* and *Karenia mikimotoi* reduce the survival and reproduction of copepod *Calanus sinicus*. J Mar Biol Assoc UK 95, 1071-1079.

Lindahl, O., 1983. On the development of a *Gyrodinium aureolum* occurrence on the Swedish west coast in 1982. Mar Biol 77, 143-150.

Lu, S., Hodgkiss, I.J., 2004. Harmful algal bloom causative collected from Hong Kong waters. Hydrobiologia 512, 231-238.

Madhu, N.V., Reny, P.D., Paul, M., Ullas, N., Resmi, P., 2011. Occurrence of red tide caused by *Karenia mikimotoi* (toxic dinoflagellate) in the Southwest coast of India. Indian J Geo Mar Sci 40, 821-825.

Margalef, R., 1975. Assessment of the effects on plankton., In: Pearson, E.A., Frangipane, O. (Eds.), Marine pollution and marine waste disposal. Pergamon Press, Oxford, pp. 301-306.

Masó, M., Garcés, E., Pagès, F., Camp, J., 2003. Drifting plastic debris as a potential vector for dispersing Harmful Algal Bloom (HAB) species. Sci Mar 67, 107-111.

McKinstry, C.A.E., Campbell, R.W., 2018. Seasonal variation of zooplankton abundance and community structure in Prince William Sound, Alaska, 2009–2016. Deep Sea Res Part II 147, 69-78.

MDMR, 2017. Maine Division of Marine Resources monitors unusual plankton bloom in Casco Bay. Available at: https://www.maine.gov/dmr/news-details.html?id=767409 Access date: 28 February, 2019.

Ministry of the Environment, Japanese Agency, 2012. Estimated Total Amount of Debris Washed Out by the Great East Japan Earthquake. http://www.env.go.jp/en/focus/docs/files/20120901-57.pdf, Access date: 7 October 2019.

Mitchell, S., Rodger, H., 2007. Pathology of wild and cultured fish affected by a *Karenia mikimotoi* bloom in Ireland, 2005. Bull Eur Assoc Fish Pathol 27, 39-42.

Mooney, B.D., Dorantes-Aranda, J.J., Place, A.R., Hallegraeff, G.M., 2011. Ichthyotoxicity of gymnodinioid dinoflagellates: PUFA and superoxide effects in sheepshead minnow larvae and rainbow trout gill cells. Mar Ecol Prog Ser 426, 213-224.

Murray, C.C., Maximenko, N., Lippiatt, S., 2018. The influx of marine debris from the Great Japan Tsunami of 2011 to North American shorelines. Mar Poll Bull 132, 26-32.

Nakamura, Y., Suzuki, S., Hiromi, J., 1995. Population dynamics of heterotrophic dinoflagellates during a Gymnodinium mikimotoi red tide in the Seto Inland Sea. Mar Ecol Prog Ser 125, 269-277.

Nakamura, Y., Suzuki, S., Hiromi, J., 1996. Development and collapse of a *Gymnodinium mikimotoi* red tide in the Seto Inland Sea. Aquat Microb Ecol 10, 131-137.

Nakano,T., Adachi, R., Hirooka, S., Tominaga, H., 1987. *Gymnodinium nagasakiense* a red-tide forming dinoflagellate, and its culture medium. La Mer 25,104-108.

Nishibori, N., Imai, I., 2013. Polyamines control the growth of the fish-killing dinoflagellate *Karenia mikimotoi* in culture. Harmful Algae 29, 10-13.

O'Boyle, S., McDermott, G., Silke, J., Cusack, C., 2016. Potential impact of an exceptional bloom of *Karenia mikimotoi* on dissolved oxygen levels in waters off western Ireland. Harmful Algae 53, 77-85.

Oda, M., 1935. *Gymnodinium mikimotoi* Miyake et Kominami n. sp. (MS.) no akashiwo to ryusando no koka (The red tide of *Gymnodinium mikimotoi* Miyake et Kominami n. sp. (MS) and the influence of copper sulfate on the red tide). Zoology Magazine 47, 35-48.

Okkonen, S.R., Pegau, S., Saupe, S.M., 2009. Seasonality of boundary conditions for Cook Inlet, Alaska. OCS Study MMS 2009-041. Department of the Interior, Minerals Management Service and University of Alaska Fairbanks, Univeristy of Alaska. Fairbanks, AK. 64 pp.

Paerl, H.W., 1988. Nuisance phytoplankton blooms in coastal, estuarine, and inland waters. Limnol Oceanogr 33, 823-843.

PIRSA, 2014. Fish kill investigation: Coffin Bay harmful algal (*Karenia mikimotoi*) bloom February 2014. Primary Industries and Resources South Australia (PIRSA), Fisheries and Aquaculture Division. Adelaide, Australia. pp. 33.

Poot-Delgado, C.A., Okolodkov, Y.B., Aké-Castillo, J.A., Rendón-von Osten, J., 2015 Annual cycle of phytoplankton with emphasis on potentially harmful species in oyster beds of Términos Lagoon, southeastern Gulf of Mexico. Rev Biol Mar Oceanogr 50, 465-477.

Qurban, M.A., 2009. An investigation of factors influencing the spatial and temporal distribution of surface phytoplankton in the English Channel and Bay of Biscay in 2003 and 2004. University of Southampton, School of Ocean and Earth Sciences, PhD Thesis, 199 pp.

Raine, R., O'Boyle, S., O'Higgins, T., White, M., Patching, J., Cahill, B., McMahon, T., 2001. A satellite and field portrait of a *Karenia mikimotoi* bloom off the south coast of Ireland, August 1998. Hydrobiologia 465, 187-193.

Robin, R.S., Kanuri, V.V., Muduli, P.R., Mishra, R.K., Jaikumar, M., Karthikeyan, P., Suresh Kumar, C., Saravana Kumar, C., 2013. Dinoflagellate Bloom of *Karenia mikimotoi* along the Southeast Arabian Sea, Bordering Western India. J Ecosys 2013, 11.

Satake, M., Shoji, M., Oshima, Y., Naoki, H., Fujita, T., Yasumoto, T., 2002. Gymnocin-A, a cytotoxic polyether from the notorious red tide dinoflagellate, *Gymnodinium mikimotoi*. Tetrahedron Lett 43, 5829-5832.

Satake, M., Tanaka, Y., Ishikura, Y., Oshima, Y., Naoki, H., Yasumoto, T., 2005. Gymnocin-B with the largest contiguous polyether rings from the red tide dinotlagellate, *Karenia* (formerly *Gymnodinium*) *mikimotoi*. Tetrahedron Lett 46, 3537-3540.

Sathish Kumar, P., Kumaraswami, M., Durga Rao, G., Ezhilarasan, P., Sivasankar, R., Ranga, V., Rao, Ramu, K., 2018. Influence of nutrient fluxes on phytoplankton community and harmful algal blooms along the coastal waters of southeastern Arabian Sea. Cont Shelf Res 161, 20-28.

Shen, A., Ma, Z., Jiang, K., Li, D., 2016. Effects of temperature on growth, photophysiology, Rubisco gene expression in *Prorocentrum donghaiense* and *Karenia mikimotoi* et. Ocean Sci J 51, 581.

Shi, F., McNabb, P., Rhodes, L., Holland, P., Webb, S., Adamson, J., Immers, A., Gooneratne, R., Holland, J., 2012. The toxic effects of three dinoflagellate species from the genus *Karenia* on invertebrate larvae and finfish. New Zeal J Mar Fresh 46, 149-165.

Shikata, T., Matsunaga, S., Nishide, H., Sakamoto, S., Onistuka, G., Yamaguchi, M., 2015. Diurnal vertical migration rhythms and their photoresponse in four phytoflagellates causing harmful algal blooms. Limnol Oceanogr 60, 1251-1264.

Shikata, T., Onitsuka, G., Abe, K., Kitatsuji, S., Yufu, K., Yoshikawa, Y., Honjo, T., Miyamura, K., 2017. Relationships between light environment and subsurface accumulation during the daytime in the red-tide dinoflagellate *Karenia mikimotoi*. Mar Biol 164, 18.

Shimada, H., Kanamori, M., Yoshida, H., Imai, I., 2016. First record of red tide due to the harmful dinoflagellate *Karenia mikimotoi* in Hakodate Bay, southern Hokkaido, in autumn 2015. Nippon Suisan Gakk 82, 934-938.

Silke, J., O'Beirn, F., Cronin, M., 2005. *Karenia mikimotoi*: An Exceptional Dinoflagellate Bloom in Western Irish Waters, Summer 2005. Marine Environment and Health Series, No 21. Marine Institute Marine Environment and Food Safety Services Galway. 1-48.

Smayda, T.J., 1980. Phytoplankton species succession, In: Morris, I. (Ed.), The physiologoical ecology of phytoplankton. Blackwell Scientific Publ., Boston, pp. 493-570.

Smayda, T.J., 2007. Reflections on the ballast water dispersal—harmful algal bloom paradigm. Harmful Algae 6, 601-622.

Smith, K.F., de Salas, M., Adamson, J., Rhodes, L.L., 2014. Rapid and accurate identification by real-time PCR of biotoxin-producing dinoflagellates from the family Gymnodiniaceae. Marine drugs 12, 1361-1376.

Song, S., Li, Z., Li, C., Yu, Z., 2017. The response of spring phytoplankton assemblage to diluted water and upwelling in the eutrophic Changjiang (Yangtze River) Estuary. Acta Oceanol Sin 36, 101-110.

Sourisseau, M., Jegou, K., Lunven, M., Quere, J., Gohin, F., Bryere, P., 2016. Distribution and dynamics of two species of Dinophyceae producing high biomass blooms over the French Atlantic Shelf. Harmful Algae 53, 53-63.

Sournia, A., 1982. Form and function in marine phytoplankton. Biol Rev 57, 347-394.

Thompson, J.D., Gibson, T.J., Plewniak, F., Jeanmougin, F., Higgins, D.G., 1997. The ClustalX windows interface: flexible strategies for multiple sequence alignment aided by quality analysis tools. Nucleic Acids Res 24, 4876-4882.

Vandersea, M.W., Kibler, S.R., Holland, W.C., Tester, P.A., Schultz, T.F., Faust, M.A., Holmes, M.J., Chinain, M., Wayne Litaker, R., 2012. Development of semi-quantitative PCR assays for the detection and enumeration of *Gambierdiscus* species (Gonyaulacales, Dinophyceae). J Phycol 48, 902-915.

Vandersea, M.W., Kibler, S.R., Tester, P.A., Holderied, K., Hondolero, D.E., Powell, K., Baird, S., Doroff, A., Dugan, D., Litaker, R.W., 2018. Environmental factors influencing the distribution and abundance of *Alexandrium catenella* in Kachemak bay and lower cook inlet, Alaska. Harmful Algae 77, 81-92.

Vandersea, M.W., Kibler, S.R., Van Sant, S.B., Tester, P.A., Sullivan, K., Eckert, G., Cammarata, C., Reece, K., Scott, G., Place, A., Holderied, K., Hondolero, D., Litaker, R.W., 2017. qPCR assays for *Alexandrium fundyense* and *A. ostenfeldii* (Dinophyceae) identified from Alaskan waters and a review of species-specific *Alexandrium* molecular assays. Phycologia 56, 303-320.

Videau, C., Partensky, F., 1990. Variability in the growth characteristics of *Gymnodinium* cf. *nagasakiense* (Dinophyceae) and its consequences for the determination of in situ growth rates. J Exper Mar Biol Ecol 142, 169-182.

Widdicombe, C.E., Eloire, D., Harbour, D., Harris, R.P., Somerfield, P.J., 2010. Long-term phytoplankton community dynamics in the Western English Channel. J Plankton Res 32, 643-655.

Yamaguchi, M., Honjo, T., 1989. Effects of temperature, salinity and irradiance on the growth of the noxious red tide flagellate *Gymnodinium nagasakiense* (Dinophyceae). Nippon Suisan Gakk 55, 2029-2036.

Yamaguchi, M., Itakura, S., 1999. Nutrition and growth kinetics in nitrogen- or phosphorus-limited cultures of the noxious red tide dinoflagellate *Gymnodinium mikimotoi*. Fisheries Sci 65, 367-373.

Yuan, J., Mi, T., Zhen, Y., Yu, Z., 2012. Development of a rapid detection and quantification method of *Karenia mikimotoi* by real-time quantitative PCR. Harmful Algae 17, 83-91.

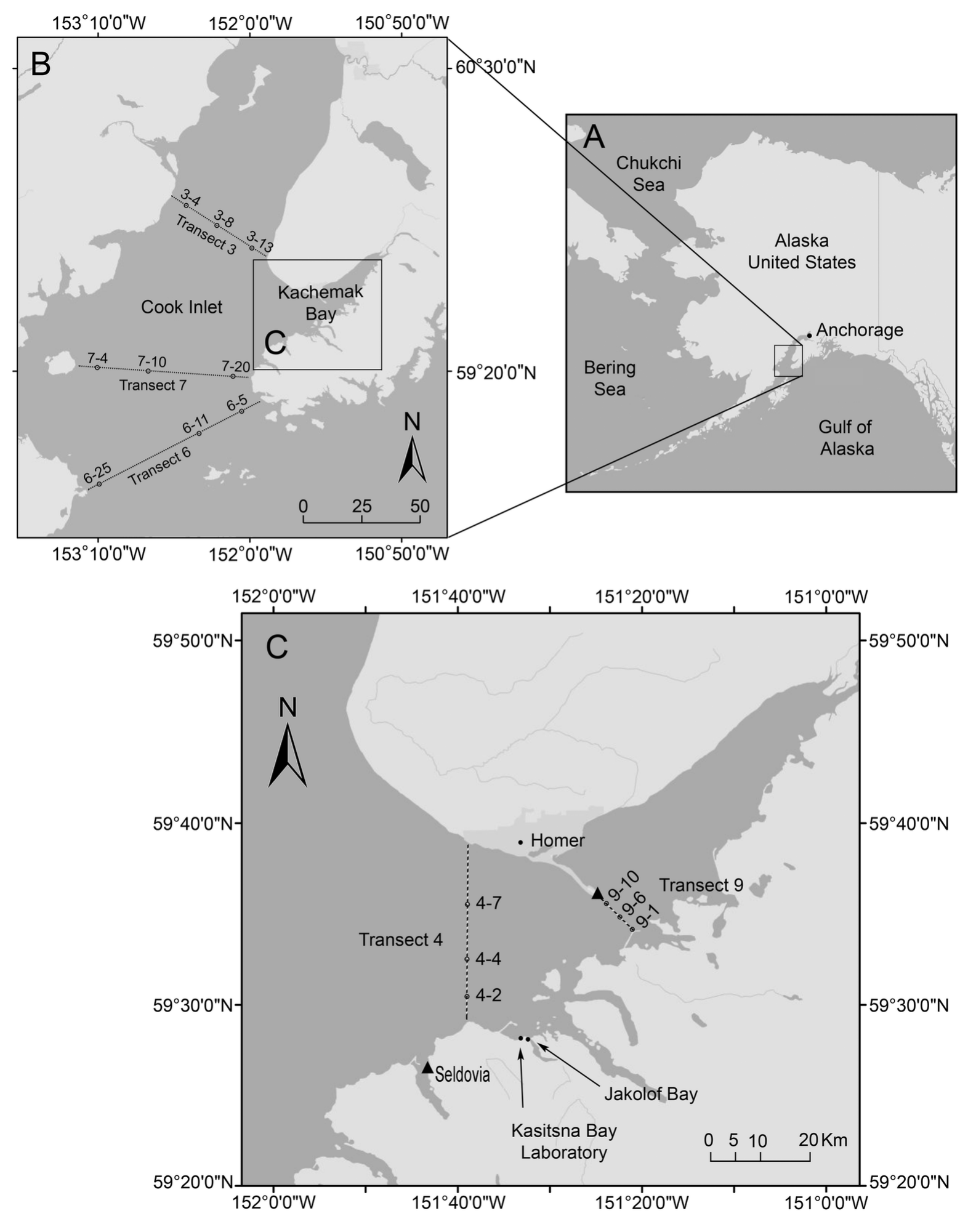
B
153°10'0"W
152°0'0"W
150°50'0"W
60°30'0"N
59°20'0"N
3-4
3-8
3-13
Transect 3
Cook Inlet
Kachemak Bay
C
7-4
7-10
7-20
Transect 7
6-5
6-11
6-25
Transect 6
N
0 25 50
A
Chukchi Sea
Alaska United States
Anchorage
Bering Sea
Gulf of Alaska
152°0'0"W
151°40'0"W
151°20'0"W
151°0'0"W
59°50'0"N
59°40'0"N
59°30'0"N
59°20'0"N
C
N
Homer
9-10
9-6
9-1
Transect 9
4-7
Transect 4
4-4
4-2
Seldovia
Jakolof Bay
Kasitsna Bay Laboratory
0 5 10 20 Km

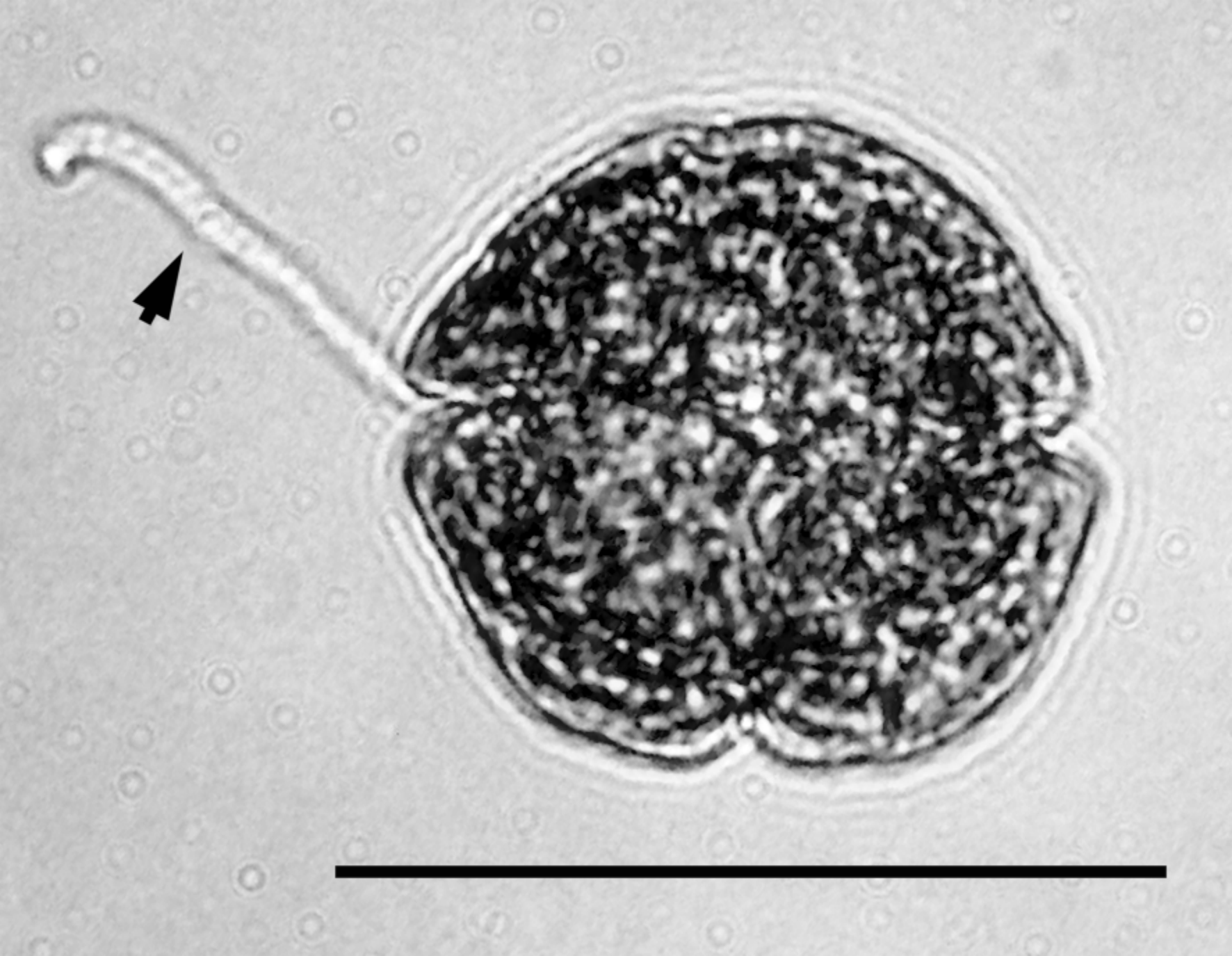

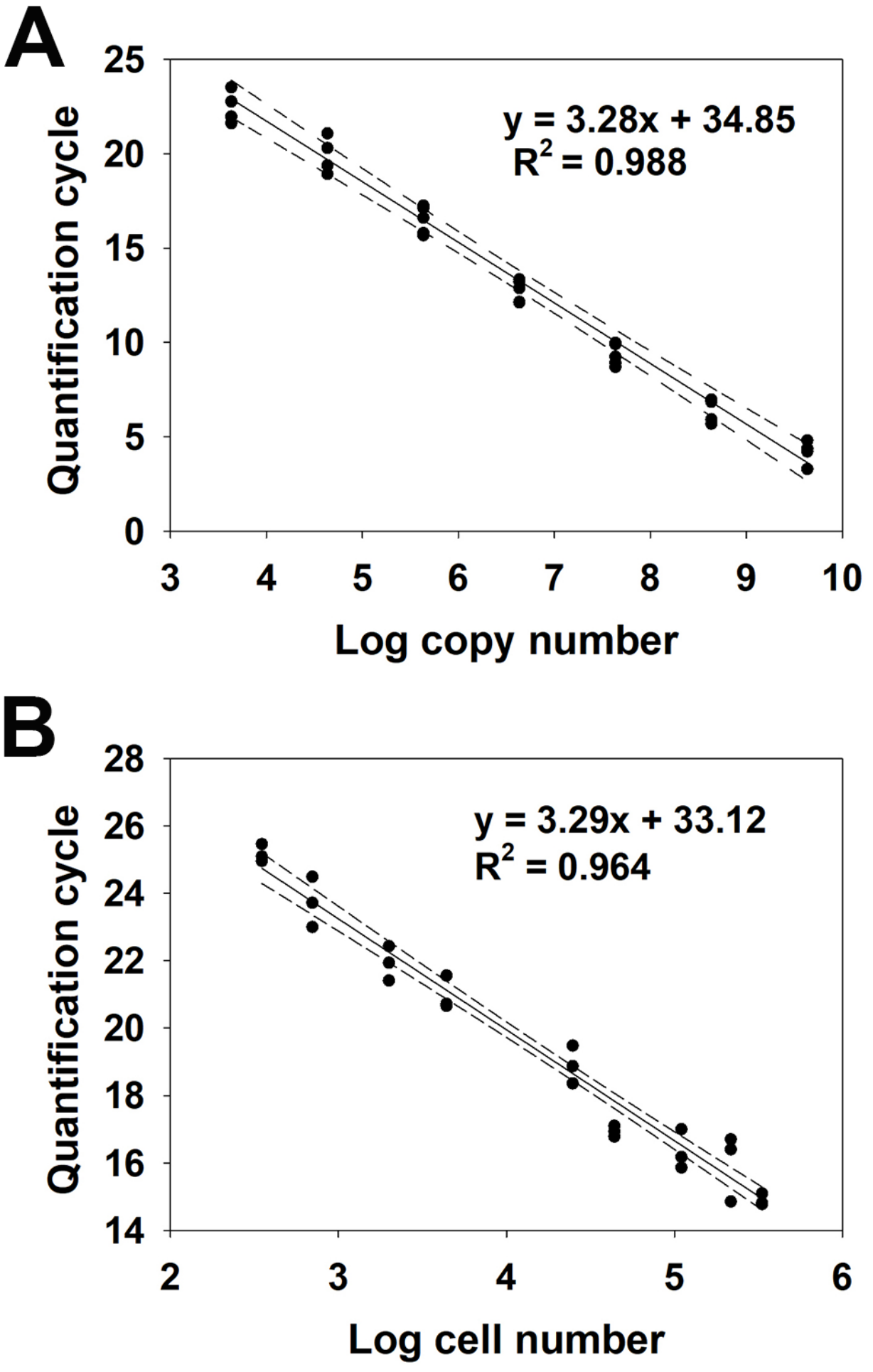
A
Quantification cycle
25
20
15
10
5
0
y = 3.28x + 34.85
R2 = 0.988
3
4
5
6
7
8
9
10
Log copy number
B
Quantification cycle
28
26
24
22
20
18
16
14
y = 3.29x + 33.12
R2 = 0.964
2
3
4
5
6
Log cell number

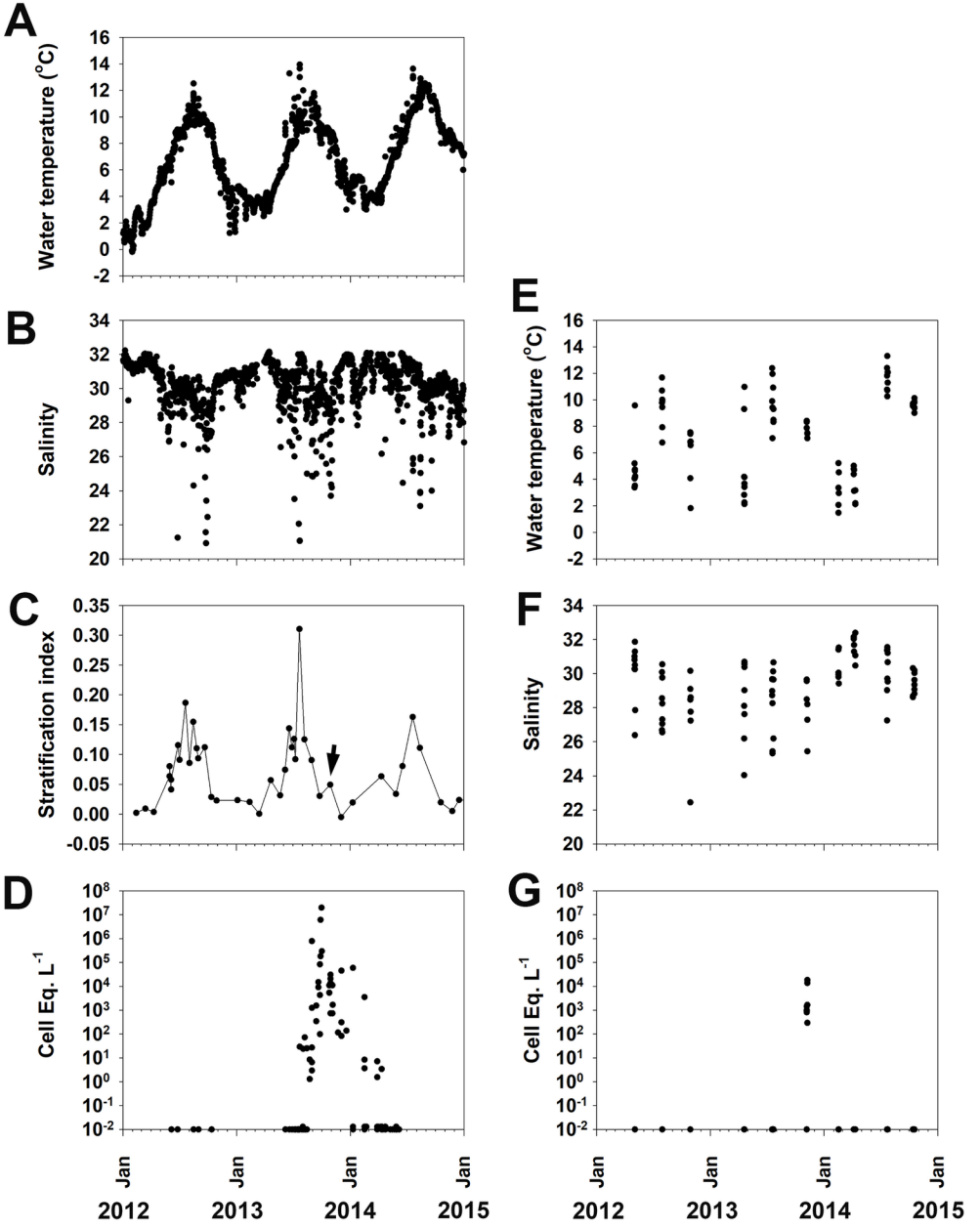
A
Water temperature (°C)
B
Salinity
C
Stratification index
D
Cell Eq. L-1
E
Water temperature (°C)
F
Salinity
G
Cell Eq. L-1
Jan
2012
2013
2014
2015

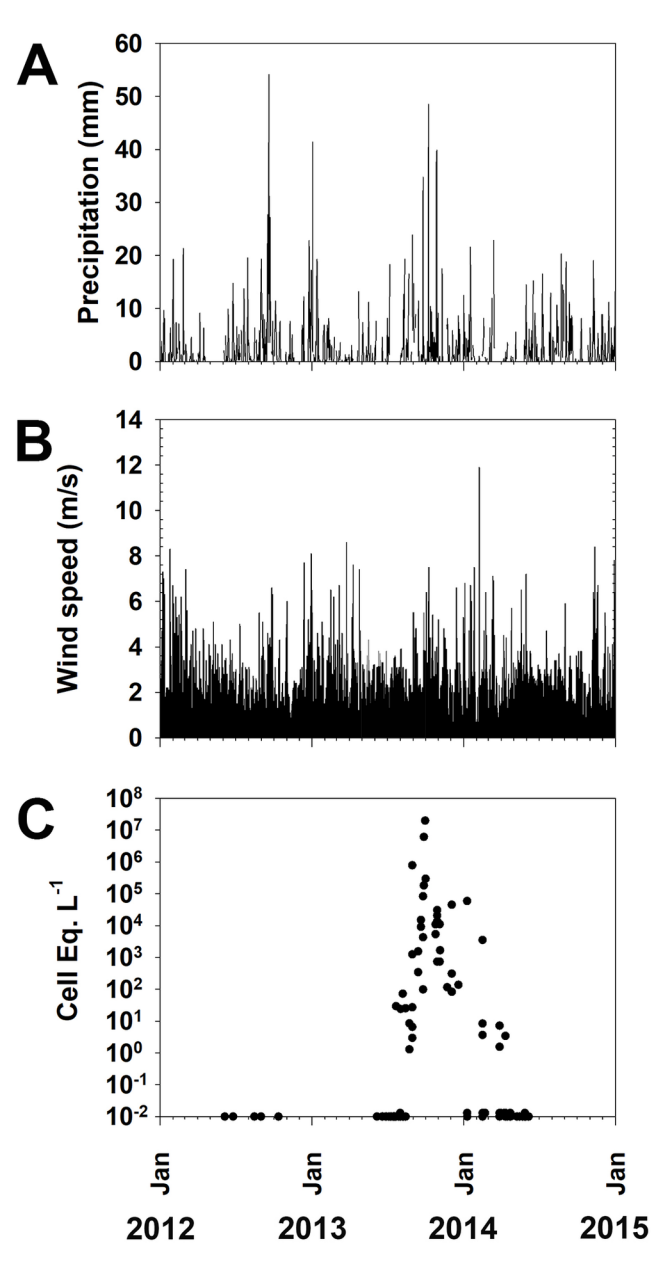
A
Precipitation (mm)
60
50
40
30
20
10
0
B
Wind speed (m/s)
14
12
10
8
6
4
2
0
C
Cell Eq. L-1
10^8
10^7
10^6
10^5
10^4
10^3
10^2
10^1
10^0
10^-1
10^-2
Jan
2012
Jan
2013
Jan
2014
Jan
2015

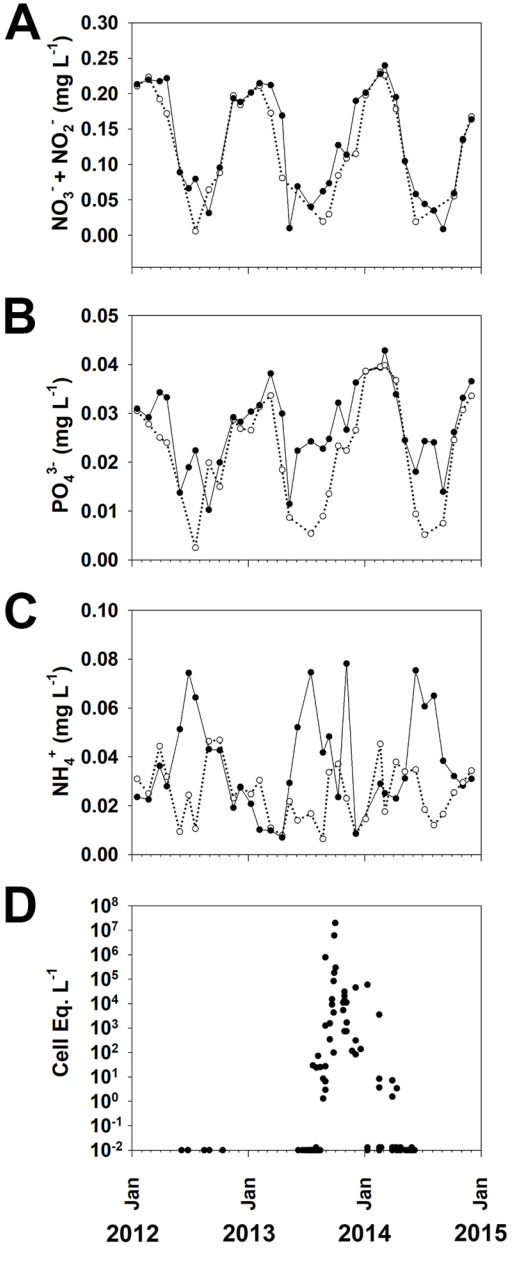
A
0.30
0.25
0.20
0.15
0.10
0.05
0.00
$NO_3^- + NO_2^-$ (mg L^{-1})
B
0.05
0.04
0.03
0.02
0.01
0.00
PO_4^{3-} (mg L^{-1})
C
0.10
0.08
0.06
0.04
0.02
0.00
NH_4^+ (mg L^{-1})
D
10^8
10^7
10^6
10^5
10^4
10^3
10^2
10^1
10^0
10^{-1}
10^{-2}
Cell Eq. L^{-1}
Jan
2012
Jan
2013
Jan
2014
Jan
2015

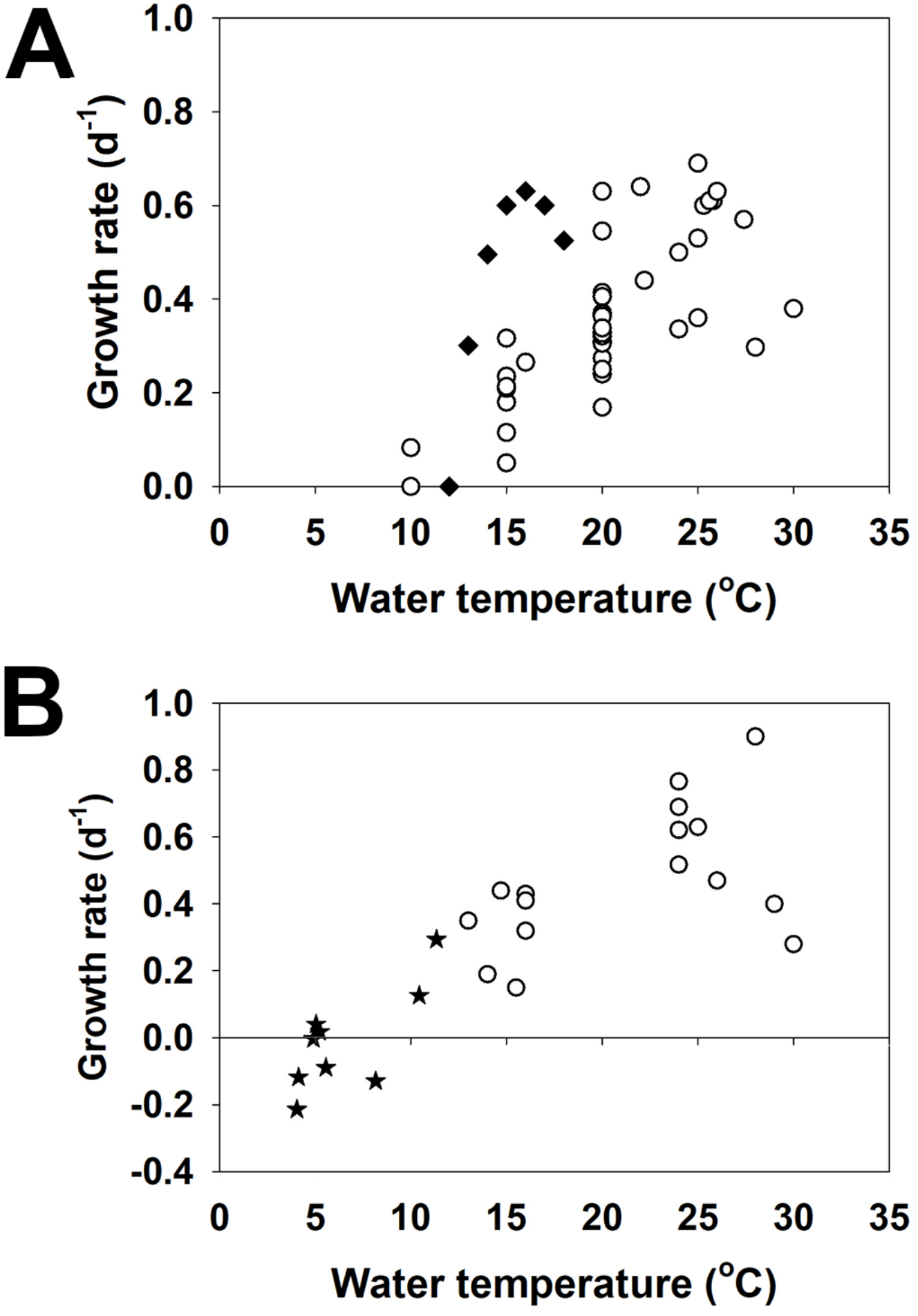
A
1.0
0.8
0.6
0.4
0.2
0.0
Growth rate (d-1)
0
5
10
15
20
25
30
35
Water temperature (°C)
B
1.0
0.8
0.6
0.4
0.2
0.0
-0.2
-0.4
Growth rate (d-1)
0
5
10
15
20
25
30
35
Water temperature (°C)

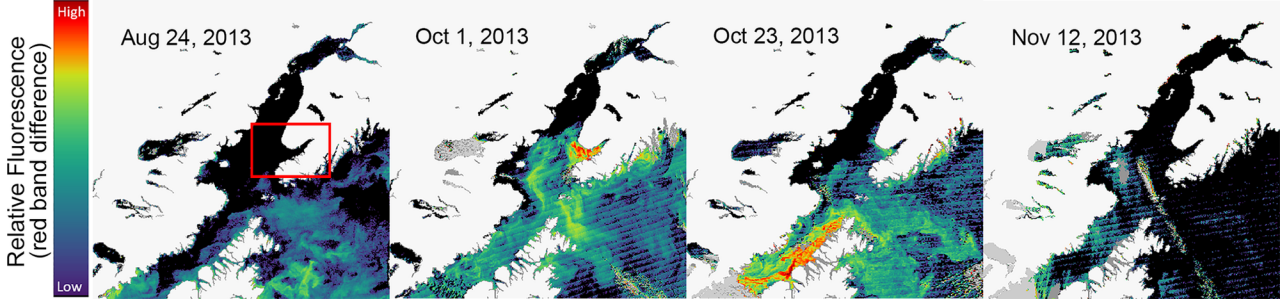
Relative Fluorescence
(red band difference)
High
Low
Aug 24, 2013
Oct 1, 2013
Oct 23, 2013
Nov 12, 2013

Table 1. Literature survey of environmental and bloom conditions of globally occurring *Karenia mikimotoi*.

Location	Cell Concentrations and Prevailing Conditions During Bloom			Range over which cells were observed		Conditions favoring bloom Formation	Reference
	K. mikimotoi (cells L^{-1})	Temperature (°C)	Salinity	Temperature (°C)	Salinity		
Kachemak Bay, Alaska, USA	1000 – 19,900,000	8 - 12	24.8 – 31.8	3 - 14	21 - 32	Stratification and nutrient rich waters accessible below thermocline	Vandersea et al this study
Imari Bay, Japan	10,000 - 10,000,000	26 - 29	32 - 34			Stratification of due to freshwater inflow coupled with upwelling induced delivery high nutrient bottom water accessible to *K. mikimotoi* and by limited water exchange	Aoki et al. 2017; Aoki et al. 2019
English Channel	200,000 - 1,500,000	12 - 17	33.9 - 35.5			Stratification due to high runoff delivering increased nutrients	Barnes et al. 2015
Gulf of Lawrence, Canada	2,000 - 990,000	12 - 13	17 - 29	4 - 19	15 - 31	Strong vertical stratification, shallow thermocline, presence of an estuarine front, and availability high ammonia concentrations	Blasco et al., 1996
Carmans Estuary, Long Island Sound, New York, USA	>1000 - 10,200,000	24.5 - 29	6 - 20	19 - 30	0 - 22	Strong vertical stratification	Chang and Carpenter, 1985
Norwegian waters	500,000 – 10,000,000	21	22.3	5 - 22	12 - 35	Blooms in stratified waters along frontal zones	Dahl and Tangen, 1993
Coast of Thiruvananthapuram, west India	2,000 - 94,000	28.2 - 28.5	33.9 - 35.7			Stratification due to heavy runoff delivering increased nutrients	Iyer et al., 2008)
English Channel	700,000-1,380,000	16 - 18.5	35.05 - 35.2			Stratification due lower salinity intrusions and calm winds	Hartman et al., 2014
English Channel	69,000 - 2,649,000	12.5 - 16	34.6 - 35.1			Intense stratification	Holligan et al., 1984
Gokasho Bay, Japan	1,000 - 4,500,000	12 - 27					Honjo et al., 1991; Honjo, 1994
Ria of Pontevedra, northwest Spain	8,908,000 - 69,337,000	19 - 19.5	35.02 - 35.10			Stratification and nutrient rich waters accessible below thermocline	Jiménez et al., 1992
Western English Channel	39,810 - 1,585,000	14 - 16		12 - 16		Stratification	Jordan and Joint, 1984
East Johor Straits between Peninsular Malaysia to the north and Singapore to the south	1,350,000 - 8,370,000	27.4 ± 1.41	21 - 25			Runoff decreased salinity, increased salinity and input of high levels N and P	Kok et al., 2019
Changjiang River estuary and adjacent waters, China	64,000 - 8,730,000	17.2 - 19.3	24.3 - 30.6			Correlated with reduced salinity, increased nutrient fluxes, shallow depth, and sheltered conditions	Kong et al., 2016
Sundays Estuary, South Africa	516,000	22 - 23.5	10 - 20			Stratified water column concomitant with nutrient-enriched mesohaline (~ 10m) surface waters	Lemley et al., 2018
Swedish coast	10,000 – 810,000	14 - 16	24 - 30			Strongly stratified water column; bloom develops along pycnocline where sufficient nutrients available then overtime migrates up in water column eventually forming dense surface blooms	Lindahl, 1983
Cochin inlet, Southwest coast of India	400 - 15,500,000	30.5 - 31.2	22.5 - 29.8			Thermally stratified	Madhu et al., 2011
Seto Inland Sea, Japan	2,000 - 380,000	22 - 24	30.3 - 33			Stratified, shallow thermocline (10-15 m) with accessible nutrient rich waters below thermocline	Nakamural et al., 1996
West and northwest coasts of Ireland,	5,000 - 3,700,000	13.0 - 17.1	34.2 - 34.9				O'Boyle et al., 2016
Términos Lagoon, Campeche, Mexico, SE Gulf of Mexico	1,000 - 9,000	27.8 - 28.4	17.4 - 19.5	27.8 - 30.6	11.6 - 19.5	Shallow water column (ave. 3.5 m), no vertical stratification, but low winds and abundant nutrients	Poot-Delgado et al., 2015
English Channel	5,000 - 8,000,000	19 - 22	34.8 - 35.0	12 - 22.5	34.6 - 35.8	Stratification due to unusually high summertime water temperatures >19C, favorable winds, and intrusion low salinity water from French rivers into the English Channel	Qurban, 2009
Southwestern Ireland	1,000 - 530,000	16	35.0	14.5 - 16	35.1 - 35.4	Strong thermal stratification and favorable wind stress - brought nutrient replete cells from sub-surface maxima along thermocline of waters in the northern Celtic Sea nearer surface where conditions more favorable or growth.	Raine et al., 2001
Southeast Arabian Sea, bordering western India	189,400 -193,700	28.2 - 28.5	33.9 - 35.7			Formed in thermally stratified cyclonic eddies when windspeeds (turbulence) were low but still sufficient to cause onshore accumulation in an embayment where runoff from heavy rainfall supplied nutrients	Robin et al., 2013
Southeastern Arabian Sea, India	600,000	24.2 - 27.0	33.6 - 34.8			Formed just outside inlets in stratified water formed from outflow of N-rich water from the inlets during summer monsoon	Sathish Kumar et al., 2018
Hiroshima Bay, Japan	1000 - >10,000,00	22.5 - 24.8	27.2 - 30.5	22.2 - 27.0	21.3 - 31.0	Highly stratified	Shikata etal., 2017
Changjiang (Yangtze River) Estuary, China	20,000 - 909,900	18 - 22	27 - 32			Stratified stations, characterized by low nitrate, low phosphate and turbidity - dense accumulation cells along the isohaline with access to nutrients below	Song et al., 2017